

Numerical Analysis of Axial Capacity and Ductility of RC Thin-Section Columns with Various Hoop's Configurations

I Ketut Sudarsana^{1*} and I Gede Gegiranang Wiryadi²

¹Department of Civil Engineering
Engineering Faculty, Udayana University
Badung, 80361, Bali, Indonesia
ksudarsana@unud.ac.id

²Department of Civil Engineering
Engineering Faculty, Mahasaraswati Denpasar University
Denpasar, 80233, Bali, Indonesia
gegiranangwiryadi@unmas.ac.id



Abstract— This numerical study is done to evaluate the effect of confinement on the axial capacity and ductility of thin section columns using the plastic damage plasticity (CDP) model in Abaqus. Seven specimens of short columns with the size of 100x400x300 mm subjected to uniaxial compression loads were analyzed based on material parameters and modeling technics that were first validated using an experimental specimen. The variation in confinement was made by changes in the configurations of the column hoops giving the variation on the hoops volumetric ratios such as 1,06% (C1), 1,16% (C2), 1,25% (C3), 1,34% (C4), 1,69% (C5), 1,25% (C6) and 2,02% (C7). All specimen models have longitudinal rebars of 10D13 ($A_s = 1327 \text{ mm}^2$) and hoops $\varnothing 5.6$ with a yield strength of 437 MPa and 284 MPa, respectively. The compressive concrete strength of 21,5 MPa was considered according to the tested specimen for validation. The validated results show that the finite element analysis can predict well the behaviors of the tested column specimen in terms of stress on concrete, reinforcement, and the crack pattern. The analysis results of the hoops parameters show that increasing the hoops' volumetric ratio can increase the capacity of the concrete core but not the column's ductility. The maximum increase in the column capacity of 87.15% occurs in specimen C4 with the hoops volumetric ratio of 1,34% and the lowest of 58.14% occurs in specimen C3 with the hoops volumetric ratio of 1,25%. The specimen model C7 with the highest hoops volumetric ratio of 2.02% increases the capacity by only 65.27%. The effectiveness of confinement is not only determined by the higher values of the hoops' volumetric ratio but also by the proper configurations of the hoops to obtain effective confining effects on the concrete core.

Keywords— Thin column section, confinement, finite element analysis, capacity, ductility

I. INTRODUCTION

Columns are structural elements that support the whole structure vertically. Based on the slenderness of the column, columns can be divided into short and slender columns [1]. The slenderness of the column is inversely proportional to the radius of gyration of the cross-section, so the thin section columns tend to behave as slender columns, especially with deformation towards the weak axis of the section [2]. In addition, columns with a thin cross-section have small confined concrete cores which expected portions of the column section to stay in place during inelastic behavior to guarantee column ductility [3]. Therefore, it is necessary to investigate the effectiveness of the hoops in restraining the concrete cores of the thin section columns, hence the columns' ductility through the confining effects [4], [5].

Codes of practice (ACI 318 and SNI 3847) require the column sections for an earthquake-resistant structure having the shortest column cross-section of 300mm and the minimum ratio of short-to-long cross-section of 0.3 [1], [6]. Meanwhile, thin column sections have a ratio of short to long sides less than 0.3, and mostly the short side of the column section is less than 300 mm. These types of columns are commonly used in a two to three-reinforced concrete building in high seismic risks i.e., Bali Island. This condition makes the selection of thin columns as structural elements must be evaluated to guarantee the effective confinement obtained and hence the columns' ductility.

A good confinement of stirrups or hoops can increase the capacity and ductility of the columns since it can maintain the concrete core when an overload occurs. Several concrete confinement models have been proposed in the literature to show that confinement affects the strength and ductility of columns [7], [8], [9]. One of the models shown in Fig. 1 proposed by [9] indicates the changes in the stress-strain relationship of the confined concrete which can result in the compressive strength and ductility of the columns increasing significantly.

Several experimental studies have been carried out in the literature to show the effect of confinement on column ductility and capacity. The restraint forces on concrete core provided by hoops in columns are related to the increase in columns' ductility and capacity for square or rectangular column sections [5], [10], [11], even circular column sections [12], [13], [14], however, few of them have studied the effects of confinement on the thin columns. Sudarsana [3] tested short columns of the thin cross-section with uniaxial compressive loading and showed that increasing the volumetric ratio of hoops could increase the ductility of the column.

Mander [9] stated that a wide variety of confinement types are determined based on the shear and flexural reinforcement configurations to determine the effective restraint. In thin section columns where the thickness of the concrete core is small, it is possible to disturb the concrete core due to the end hook's bending of the hoops or ties, therefore further research is still needed.

Experimental testing is still a priority to get actual results, but the cost is quite expensive to test the effect of one parameter. The development of information technology both software and hardware make it possible to perform a numerical approach in investigating the effect of several parameters [15], [16], [17]. Numerical research using finite element-based software regarding column confinement has been carried out and obtained comprehensive results [18], [19]. However, most of the research is still on square columns and circular columns sections. This research still needs to be carried out to investigate the effect of confinement on thin-section columns related to their capacity and ductility since the use of thin cross-section columns is mostly recommended by an architectural design especially for low-rise residential houses even though it locates in high seismic areas.

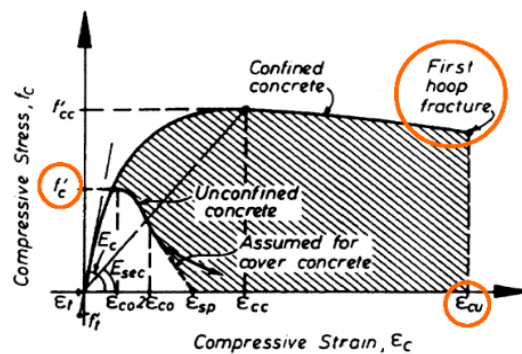


Fig. 1. Confinement model for column [9]

II. METHODS

This study has been done using a finite element (FE) based computer program, namely Abaqus® by utilizing the CDP model to model the nonlinear behavior of concrete [20]. All specimen models were analyzed following the modeling principles carried out in previous research [16], [17], [21]. The modeling parameters were previously validated using experimental tests [3] to obtain the appropriate parameter values. This is an important step so that the modeling parameters can be adjusted to the characteristics of the concrete and reinforcement materials or the test method to obtain the results of the finite element analysis match with the experimental test results [22], [23], [24].

A. Material and Specimens

All seven specimen models have the same size, namely 400mm x 100mm x 300mm, longitudinal reinforcement or flexural reinforcement using D13 mm and Ø5.6mm for transverse reinforcement or hoops. The configuration of the transverse reinforcement as a confinement can be seen in Figure 2. The compressive strength of concrete is 21.45 MPa as obtained from the test for specimen K3 used as a validation model. The reinforcing steel D13 mm and Ø5.6 mm have yield strengths of 437 MPa and 284 MPa, respectively. The validation model K3 was also included in the parametric studies and denoted as specimen C1.

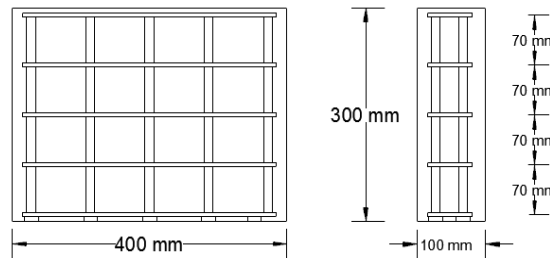


Fig. 2. Specimens dimension and hoop spacing

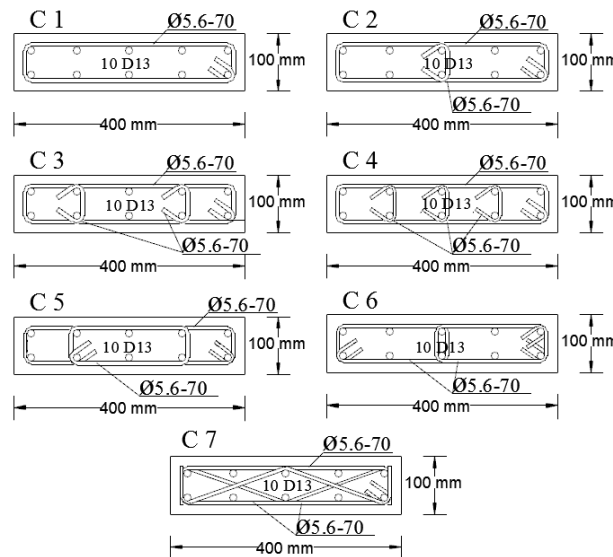


Fig. 3. Hoop rebars' configurations for confinement

Figure 2 shows the variation in types and configurations of the transverse reinforcement or stirrups in each specimen giving differences in the volumetric ratio of stirrup reinforcement (ρ_{sv}). The ratio of longitudinal reinforcement (ρ_l) remains constant for all specimens. The volumetric ratio of closed stirrups (hoops) was calculated using Equation 1 and the results for all types of specimens can be seen in Table 1. All specimens' models were subjected to axial compressive forces that act as a distributed load on one surface of the column sections while the other section was restrained.

$$\rho_{sv} = \frac{A_{st} \cdot 2(p+l)}{p \cdot l \cdot s} \times 100\% \tag{1}$$

Where ρ_{sv} is the volumetric ratio of stirrups; A_{st} is the area of the stirrups; s is a center-to-center distance of the stirrups (mm); p is the perimeter length of the confined core; l is the confined core width.

B. Modeling and Analysis

The numerical analysis uses a finite element-based program, namely Abaqus® following the modeling processes and principles that have been done previously [17], [23]. Nonlinear Concrete behavior was modeled using the concrete damage plasticity (CDP) features. Both elastic and plastic conditions of concrete were considered in the analysis. The elastic condition is defined

by the concrete modulus of elasticity (E) and poison ratio (ν). While the plastic conditions are defined by the CDP features, namely dilation angle (ψ), eccentricity (ϵ), two-way and one-way compression ratio (σ_{b0}/σ_{c0}), $K = 0.67$, viscosity parameter (μ), the compressive stress-strain concrete and tension, and the failure parameter (d) in compression and tension. Since there were no data available for the stress-strain curve of tested concrete, it follows the equation proposed by [25].

TABLE I. VOLUMETRIC RATIO OF SPECIMENS

Specimen	dimension p x l x t (mm)	Number and diameter of Longitudinal Rebar mm	Transverse Rebars mm	Volumetric Ratio of transverse rebars ρsv
C1	400x100x300	10D13	Ø5,6	1.06%
C2	400x100x300	10D13	Ø5,6	1.16%
C3	400x100x300	10D13	Ø5,6	1.25%
C4	400x100x300	10D13	Ø5,6	1.34%
C5	400x100x300	10D13	Ø5,6	1.69%
C6	400x100x300	10D13	Ø5,6	1.25%
C7	400x100x300	10D13	Ø5,6	2.02%

The concrete material is modeled in 3D elements (3D stress) called C3D8R in Abaqus. It is an 8-nodal brick element with an hourglass control integration reduction effect [17], [26]. The reinforcement bars are modeled as a 2D linear truss element-T2D3 as shown in Figure 4. Modeling reinforcement with truss elements (2D) or solid elements (3D) gives equivalent results in the linear phase [27], however, the truss elements are more efficient in terms of analysis time. The bond between the concrete and the reinforcement bars is assumed to be perfectly attached by applying the embedded region options. The mesh size used is 20 mm which is greater than the maximum aggregate size. The analysis process uses dynamics-explicit features so that the analysis can be shorter compared to the linear-static analysis because divergent increments will be skipped [20]. The axial load is applied as distributed forces to the one-end surface section of the column in the form of displacement. The other end of the column section is applied for fixed support. Reference points are placed on both surfaces of the column sections and connected to behave as a rigid body using a tie–point to surface features. These features make the surface deform simultaneously when a load or reaction acts on the reference point [20].

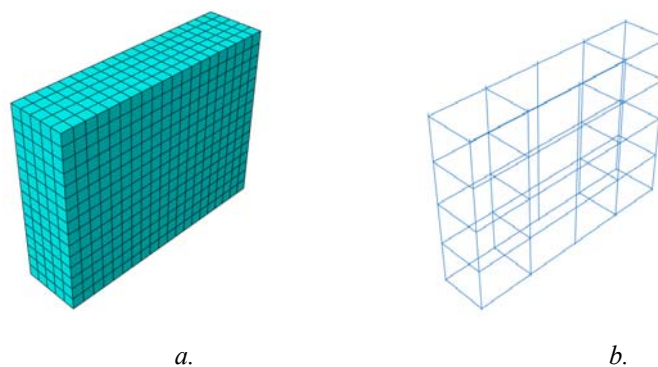


Fig. 4 Modelling material (a) Element 3D stress with mesh for concrete and (b) Element linear truss for rebar

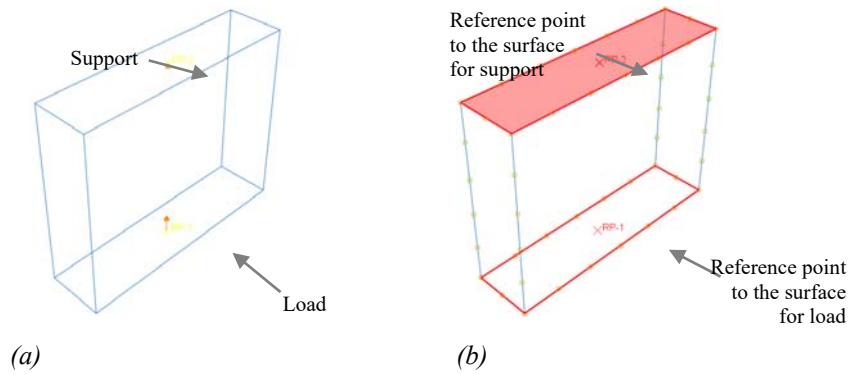


Fig. 5. Loading scheme (a) loads and supports and (b) rigid body – tie – point to surface

III. RESULTS AND DISCUSSION

C. Validating Material Parameters

The material parameters of CDP were validated using the experimental specimen data of K3 [3] which is included in this study as a specimen (C1). Considering the mesh size of 20mm, taking the reduction of concrete strength from 21.45 MPa to 16 MPa due to the reduction of the effect of the transverse tension members subjected to axial forces and the tensile strength of concrete of $0.3 \sqrt{f_c}$, it is found that the material parameters are the angle of dilation (ψ) of 30° , eccentricity (ϵ) 0.1, two-way and one-way compression ratio (σ_{b0}/σ_{c0}) 1.16, $K = 0.67$, and the viscosity parameter (μ) is 0.00001 for more accurate analysis [24]. The parameters of plastic collapse in compression (d_c) and concrete tensile (d_t) are considered.

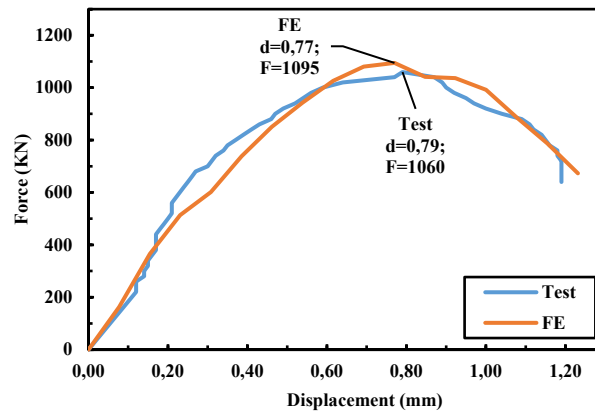


Fig. 6. Load-deformation curve for experimental test and finite element analysis

Applying all the concrete materials parameters and modeling assumptions, it is found that the numerical analysis results are in good agreement with the test results as shown in Fig. 6 for the load-deformation relationship. The peak load of the modeling results is 1095 kN while the experimental results are 1060 kN or a difference of 3.17%. The difference in axial deformation at the maximum load between the analysis and experiment results is 2.62% which is from 0.79 to 0.77 mm, respectively for the experiment and analysis.

The strain contours of the finite element analysis shown in Fig. 7 (b) are used to identify the damage of the testing specimen as given in Fig. 7 (a). It is shown that the concentration of strain contours on the top side indicates the concrete cracks or damage in the experimental specimen. In addition, the crack patterns shown in the experimental specimen are similar to the strain contours of the analysis results. Comparing the results obtained from analysis and experimental, it assumes that the modeling technique and the validated material parameters can resemble the experimental results [16], therefore will be applied to further study of hoop variations.

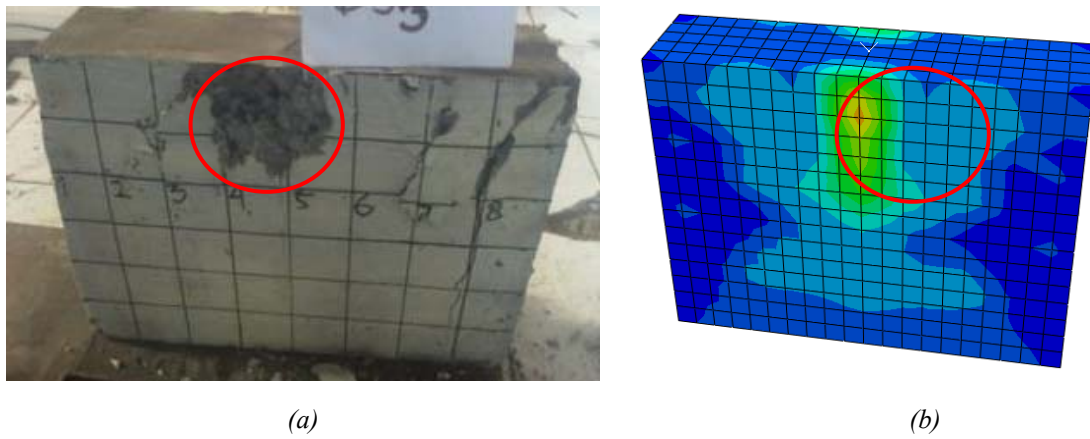


Fig. 7. Comparison crack pattern (a) experiment and (b) finite element analysis

D. Effects of Hoops Volumetric Ratios on The Column Capacity

The addition of hoops and cross ties rebars to the control specimen (C1) significantly increase the load-carrying capacity of the columns as indicated by the load-deformation relationship shown in Figure 8. At low load levels of about 500 kN, all specimens behave in the same manner as shown by the curve lines of all specimens in unity. It starts to deviate after that load indicating the commencement of the cracks until all specimens reach failure loads. Deviation of the curve is more obvious after the load reaches 1000 kN. In addition, the slope of the curve after the maximum loads vary among the specimens. These slopes indicate how fast the specimens fail or in other words how the ductility of the specimens is. The load-deformation relationship of all specimens tends to follow the model [8].

A comparison of the increase in the load capacity due to confining effects is made by comparing the capacity of the concrete core without considering the longitudinal reinforcement [7] using Equation (2) and Equation (3) as follows:

$$P_{0core} = \alpha \cdot f'_c \cdot (A_{core} - A_s) \tag{2}$$

$$P_{cmax} = P_{test} - A_s \cdot f_y \tag{3}$$

where P_{0core} is the concrete core capacity, P_{cmax} is the maximum concrete core capacity only without considering the contribution of the longitudinal reinforcement capacity, and P_{test} is the maximum force from the results of the analysis on the specimen. A_{core} and A_s are the cross-sectional areas of the column cores and the longitudinal reinforcement areas, respectively. The concrete compressive strength f'_c and the rebar yield strength f_y are considered in the analysis.

The comparison of the axial capacity of all specimens calculated following Equations (2) and (3) are given in Table 1 and the tested maximum loads are plotted in Fig. 8 for further clarity on the effects of volumetric ratios. Specimen C4 with a hoops volumetric ratio of 1.3426% exhibits the largest increase in the axial capacity of 87.15%. Specimen C4 can resist the maximum axial force of 1399 kN or 187.15% of the maximum capacity of specimen C1 which is 1095 kN. However, specimen C7 with the largest volumetric ratio ($\rho_{sv} = 2.02\%$) has an axial load carrying capacity of 1303 KN or 165.27% of the maximum capacity of the C1 specimen. Table I and Fig. 9 (a) show that increasing the hoops' volumetric ratio does increase the capacity ratio greater than 40.45% comparing data of specimens C1 and C3. However, the effect of an increase in hoops volumetric ratio obtained for different configurations as shown in Fig. 3 for thin section columns does not increase the axial capacity of the column significantly. The most effective hoop configuration to the axial capacity is given by specimen C4 having cross ties for all longitudinal reinforcement. This may restrain the expansion of the concrete core. The analysis results also show that the effective restraint to increase the column capacity depends on the confinement configuration but not only based on the increasing the hoops volumetric ratios. The analysis results found in this study are following previous studies from other researchers that show the effectiveness of the confinement is not only adding the reinforcement volume but also its configurations need to have attention [4], [28].

E. Effects of Hoops Volumetric Ratios on The Column Ductility

The axial ductility of all specimens is measured and analyzed based on strain ductility. It is calculated by comparing the strain at collapse load ($0.85 P_{max}$) with the strain at maximum load (P_{max}) as presented in Table 2 and Fig. 9 (b). The analysis results show

that the control specimen C1 with a volumetric ratio (ρ_{sv}) of 1.064% has the highest strain ductility of 1.357, among others. The lowest one is shown by specimen C3 with the $\rho_{sv} = 1.059\%$. The results for the strain ductility show different trends with the specimen capacity in which increasing the hoops' volumetric ratio by adding cross ties or another hoop does not increase the axial strain ductility. This ductility behavior of the thin section columns may be due to the disturbance of the concrete core by hoops hooks and cross ties rebars which causes the concrete core to experience premature cracks. The load-displacement curves shown in Figure 8 indicate the decrease in the ductility in which the slope of the curve after reaching the maximum forces are sharper than that of specimen C1 with the increase in hoops volumetric ratios. The finding results of this study on the ductility of the thin section columns are not the same trends as the other studies [29] where the concrete core of the column sections has enough space to accommodate the hoop hooks or the cross ties rebars.

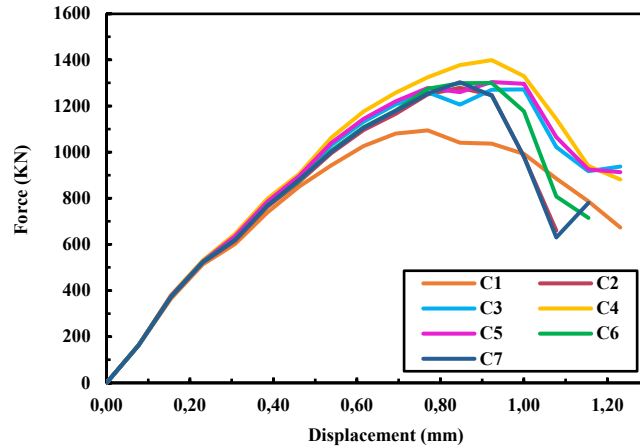


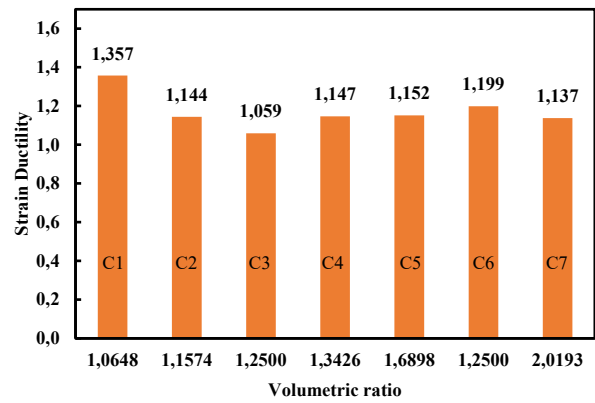
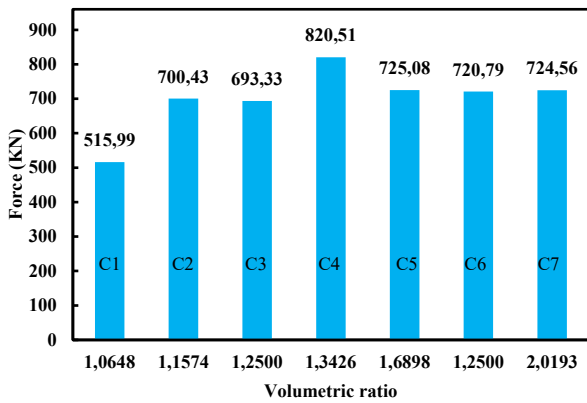
Fig. 8. Load-displacement curve of confinement effect

TABLE II. Capacity ratio

Specimens	Maximum Loads (P) kN	Displacement mm	Volumetric ratio (ρ_{sv}) %	$P_{o\ core}$ kN	$P_{c\ max}$ kN	$P_{c\ max} / P_{o\ core}$	Increases capacity ratio %
C1	1095	0.770	1.0648	438.42	515.99	1.177	17.69
C2	1279	0.847	1.1574	438.42	700.43	1.598	59.76
C3	1272	1.000	1.2500	438.42	693.33	1.581	58.14
C4	1399	0.923	1.3426	438.42	820.51	1.872	87.15
C5	1304	0.923	1.6898	438.42	725.08	1.654	65.38
C6	1300	0.847	1.2500	438.42	720.79	1.644	64.41
C7	1303	0.847	2.0193	438.42	724.56	1.653	65.27

TABLE III. Strain-ductility

Specimens	Maximum Loads (P) KN	85% max load (P)	Displacement mm	Volumetric ratio (ρ_{sv}) %	Strain max ϵ_l	The strain on 85% max. load ϵ_{85}	Strain-ductility ϵ_{85}/ϵ_l
C1	1095	901.0	0.770	1.0648	0.0026	0.00348	1.35740
C2	1279	930.5	0.847	1.1574	0.0028	0.00323	1.14426
C3	1272	1087.3	1.000	1.2500	0.0033	0.00353	1.05904
C4	1399	1081.2	0.923	1.3426	0.0031	0.00353	1.14651
C5	1304	1189.3	0.923	1.6898	0.0031	0.00354	1.15166
C6	1300	1108.2	0.847	1.2500	0.0028	0.00338	1.19892
C7	1303	1104.6	0.847	2.0193	0.0028	0.00321	1.13720



(a) (b)
Fig. 9. Effect of volumetric ratio (a) on capacity and (b) on strain ductility

F. Effects of Hoops Configuration

The specimens C2, C3, and C4 have hoop configurations by adding cross ties rebars to increase volumetric stirrups. The results of the analysis show that the load-carrying capacity increases with the addition of volumetric stirrups with the highest one in specimen C4. It also increases the ductility of specimen C4 compared to specimens C2 and C3 as the number of cross ties increased. Although its ductility is still lower than that of specimen C1.

The variation of the hoop configurations as confinement on specimens C5 and C6 is a combination of two hoops with a stirrup volumetric ratio of 1.68% and 1.25%, respectively. The capacity of specimen C5 is higher than that of specimen C6 specimen due to having larger hoops volumetric ratio, however, its ductility is a bit less than that of specimen C6.

Specimen C7 has a configuration of hoops and diagonal reinforcement in cross-section giving the largest volumetric ratio compared to the other specimens. Fig. 9 shows that the increase in the load capacity of specimen C7 was 65.27% and the ductility was 1.13. Although specimen C7 acquires the biggest hoops volumetric ratio, the highest increase in capacity is given by specimen C4 which is 87.15% with a comparable value of ductility. In terms of strain ductility, the hoop configuration of specimen C6 has the largest strain ductility of 1.199 compared to specimens C2, C3, C4, C5, and C7. These results also clearly indicate the effect of the disturbance on the concrete core by hoops hooks and cross ties rebars which causes premature cracks in the concrete core.

In this analysis study of thin section column, in terms of the axial capacity, the hoops configuration with the addition of cross ties across the column cross-section as in specimen C4 is the most effective giving the capacity increases of 87.15% although its hoops volumetric ratio of 1.3426%. The increase in hoops' volumetric ratio by adding cross ties across the column cross-section is more effective than by adding hoops and diagonal reinforcement configurations as comparing the results of specimen C4 with that one of specimens C5, C6, and C7. However, the greatest strain ductility was obtained on specimen C6. Specimens C3 and C6 have the same volumetric ratio of 1.25%, but the increase in capacity and ductility is greater than that of specimen C6. The confinement configuration for test object C7 with the largest volumetric ratio is less effective than the configuration for test objects C4 and C6.

G. Stress Distribution Patterns on Concrete

The effectiveness of the hoop configurations can also be evaluated from the stress distribution patterns in all specimens. It shows a truly clear effect of the confinement by observing the difference between the stress distributions of specimens C2 to C7 and that of specimen C1 (see Fig. 11 to Fig. 13). The stress in the concrete core is greater as the closer the spacing of the cross ties in the concrete core. in addition to increasing the stress on the concrete core, it can also be observed the stress distribution on the concrete core. If the color gradations or color patterns differ significantly, it indicates that open cracks already occurred in the concrete core, however, if the color gradations are not too different, it indicates the stress on the concrete core is even and that there are no open cracks yet.

In specimen C1, the stress in the concrete core is small which indicates the specimen resists a low load as no additional stirrups pass through the concrete core. The concrete core tends to expand out due to large axial forces (poison effect) and to push the column hoops. Whereas specimens C2 to C7 show that the stress in the concrete core is not significantly different which indicates the effectiveness of the cross ties or hoops legs crossing the concrete core to hold the perimeter hoops against lateral deformation.

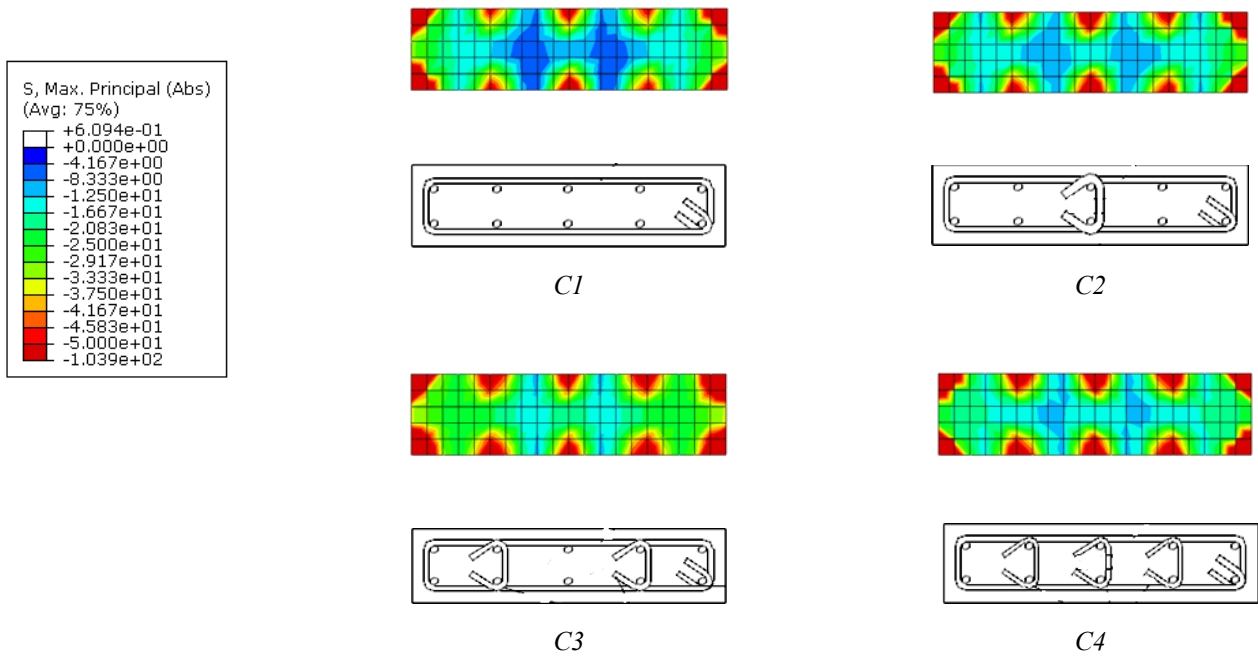


Fig. 10. Stress pattern on the section of specimens C1, C2, C3, and C4

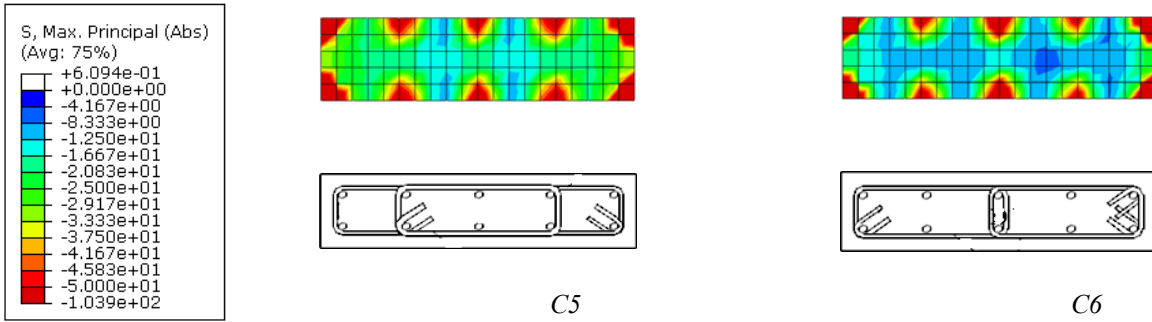


Fig. 11. Stress pattern on the section of specimens C5 and C6

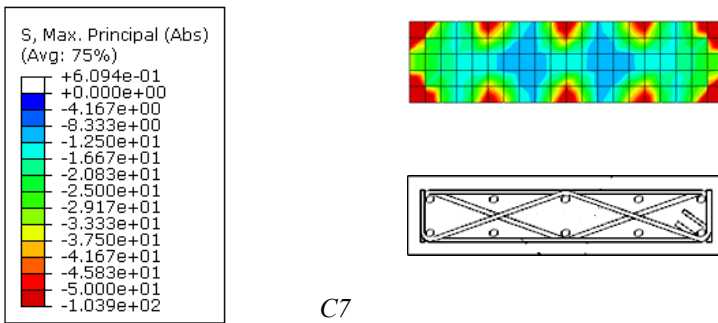


Fig. 12. Stress pattern on the section of specimen C7

H. Stress Distribution in Reinforcement

The stress in the reinforcement at the maximum loads is shown in Fig. 14 to 16, in which the longitudinal reinforcement is in compression and the transverse reinforcement is in tension. The reinforcing bars added as cross-ties going through the cross-section as in the hoop configurations specimen models C2, C3, and C4 show only the reinforcement rebars at the end of the column are still in compression, the other reinforcement rebars are in tension and reach their yield strength of 284 MPa. This is also seen in specimen C7 where the confinement configuration uses hoops and diagonal rebars crossing the column cross-section. Comparing the stress in transverse reinforcement in specimens C5 and C6 shows that some rebars in specimen C6 are in compression over the column height.

The concrete and reinforcement stresses observed in this study related to the results of the axial capacity and ductility of the specimens. It shows that the hoop configurations greatly determine the effectiveness of the confinement in increasing capacity. However, confining effects of the hoops do not work well to obtain thin column section ductility. It also can be seen from the stress distribution on the concrete and reinforcing bars as the cracks of the concrete core occurred too early.

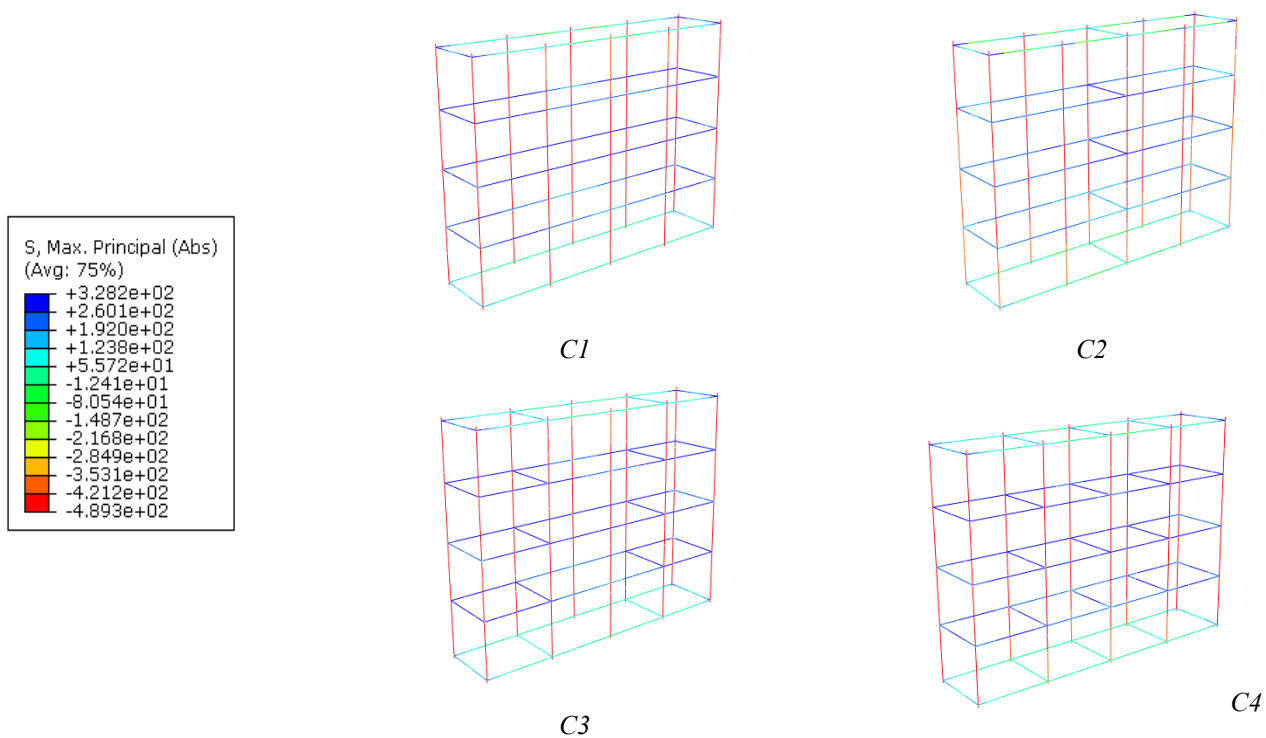


Fig. 13. Rebar stress of specimens C1, C2, C3, and C4

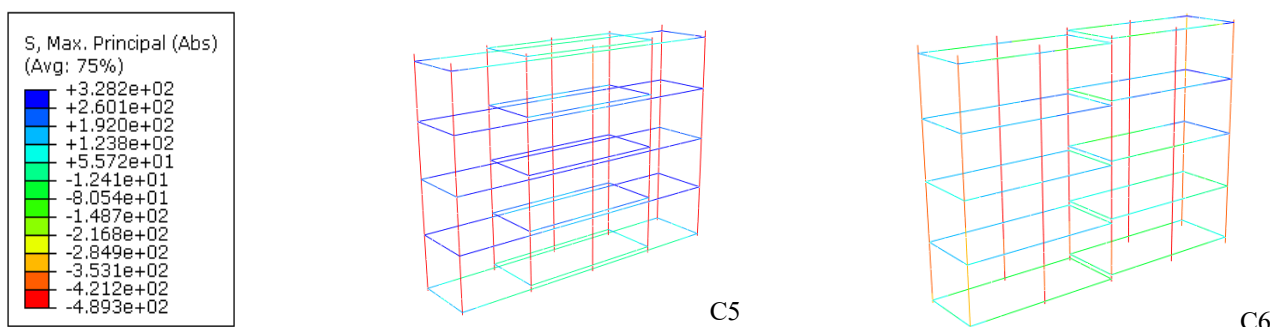


Fig. 14. Rebar stress of specimens C5 and C6

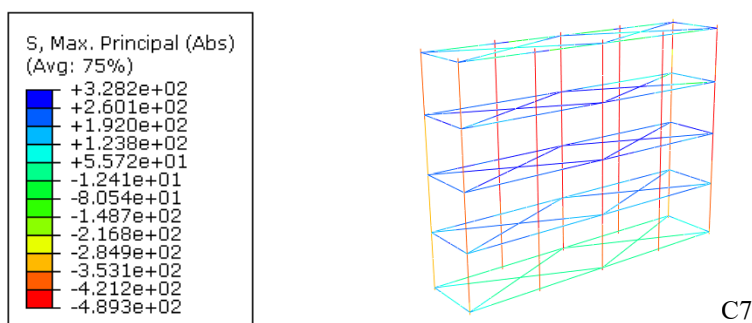


Fig. 15. Rebar stress of specimens C7

IV. CONCLUSION

The validated CDP material parameters and modeling assumption taken in this analysis give good correlated results with the experimental data in terms of load-deformation curve and strain contours to identify the experimental specimen damages. Further analysis using the validated material parameter to study the effect of hoops configurations in the thin section columns on the axial capacity and ductility shows that it cannot be only by increasing the hoops volumetric ratio to obtain the column capacity and ductility but also by its configurations as exhibited by the results of the specimen C7 although it has the higher hoops volumetric ratio of 2.0193% but giving the increase in the capacity of 65.27% Increasing the number and the volume of reinforcing bars crossing the concrete core in the form of cross ties or hoops leg of a thin section column causes premature cracks inside the concrete core, hence reducing the column capacity and ductility.

Having a hoop configuration by adding cross ties for each pair of longitudinal rebars is more effective than other types of hoop configurations. The right configurations of the hoops in the thin section column play an important role to prevent the concrete core expansion from causing premature cracks. The ductility of the specimen can also be identified by the slope of the load-deformation curve after the peak load is reached. The stiffer the slope, the less ductile the column.

The concrete stress distribution contour and the reinforcing bars can indicate the effectiveness of the hoop configuration in giving the confining effect on the concrete core. Low stress on the concrete core indicates that the concrete core is confined well or otherwise. All longitudinal reinforcement yields in compression, however, most of the transverse rebars are in tension and few of them are still in compression especially the transverse rebar at both column ends.

V. ACKNOWLEDGMENT

The authors would like to thank the Universitas Udayana and Universitas Mahasaraswati Denpasar for their support to facilitate research collaboration between the authors.

REFERENCES

- [1] Badan Standarisasi Nasional, *SNI 2847:2019 Persyaratan beton struktural untuk bangunan gedung dan penjelasan*. Jakarta, 2019, p. 695.
- [2] M. Saatcioglu, "Design of Slender Columns," in *Design Handbook (Metric)*, ACI, Ed., 2010, pp. 1–26.
- [3] I. K. Sudarsana, "Experimental study on confined concrete of thin column sections," in *Konferensi Nasional Teknik Sipil 7 (KoNTekS7)*, Solo, 2013.
- [4] S. W. N Razvi and M. G. Shaikh, "Effect of confinement on behavior of short concrete column," in *Procedia Manufacturing*, 2018.
- [5] D. De Domenico, D. Falliano, and G. Ricciardi, "Confinement effect of different arrangements of transverse reinforcement on axially loaded concrete columns: An experimental study," *J Mech Behav Mater*, vol. 28, no. 1, 2019.
- [6] ACI Committee 318, *Building Code Requirements for Structural Concrete and Commentary (ACI 318M-19)*. Farmington Hills, 2019.
- [7] M. Saatcioglu and S. R. Razvi, "Strength and ductility of confined concrete," vol. 118, no. 6, pp. 1590–1607, 1992.
- [8] D. Kent and R. Park, "Flexural members with confined concrete," 1971.
- [9] J. B. Mander, M. J. Priestley, and R. Park, "Theoretical stress-strain model for confined concrete," 1988.
- [10] Tavio Tavio, Iman Wimbadi, Ardiansyah Kusuma Negara, and Recky Tirtajaya, "Effects of confinement on interaction diagrams of square reinforced concrete columns," 2009.
- [11] J. Liu *et al.*, "Behavior of axially loaded stirrup confinement rectangular concrete-filled steel tubular stub columns," vol. 2019, 2019.
- [12] H. Karim, M. N. Sheikh, and M. N. Hadi, "Confinement of Circular Concrete Columns: A review," 2014.

- [13] S. K. Shahreza, G. Baietti, G. Quartarone, M. Santandrea, and C. Carloni, "Effect of Steel-Reinforced Grout Confinement on Concrete Square and Cylindrical Columns," *ACI Struct J*, vol. 117, no. 5, 2020.
- [14] F. Kumaseh, S. Wallah, and R. Pandaleke, "Pengaruh Jarak Senggang Terhadap Kapasitas Beban Aksial Maksimum Kolom Beton Berpenampang Lingkaran Dan Segi Empat," 2015.
- [15] I. K. Sudarsana, I. G. Gegiranang Wiryadi, and I. G. Adi Susila, "Finite element analysis of the effect M/V ratios on punching shear strength of edge slab column connections of flat plate structure," vol. 276, 2019.
- [16] I. K. Sudarsana, I. G. G. Wiryadi, and I. G. A. Susila, "Finite element analysis of punching shear-unbalanced moment interactions at edge column-flat plate connections," vol. 20, no. 1, pp. 91–100, Oct. 2022.
- [17] I. G. G. Wiryadi, I. K. D. K. Tubuh, and I. P. A. P. Wirawan, "Pemodelan Tiga Dimensi Beton Silinder yang Diuji Tekan dengan Variasi Tipe Mesh Element dan Efek Reduksi Integrasi," vol. 25, no. 1, pp. 49–56, Jan. 2021.
- [18] S. K. John, Y. Nadir, and K. Girija, "Nonlinear finite element modelling of concrete columns confined with textile reinforced mortar," in *IOP Conference Series: Earth and Environmental Science*, 2020.
- [19] S. Amirkhani and M. Lezgy-Nazargah, "Nonlinear finite element analysis of reinforced concrete columns: Evaluation of different modeling approaches for considering stirrup confinement effects," vol. 23, no. 5, 2022.
- [20] Abaqus, "Getting Started with Abaqus: Interactive Edition," in *Abaqus 6.14 Online Documentation*, USA: Dassault Systèmes Simulia, 2014.
- [21] P. Kral, P. Hradil, J. Kala, F. Hokes, and M. Husek, "Identification of the Parameters of a Concrete Damage Material Model," *Procedia Eng*, vol. 172, pp. 578–585, 2017.
- [22] F. Micelli, A. Cascardi, and M. A. Aiello, "Pre-Load Effect on CFRP-Confinement of Concrete Columns: Experimental and Theoretical Study," *Crystals (Basel)*, vol. 11, no. 2, p. 177, Feb. 2021.
- [23] I. K. Sudarsana, I. G. Gegiranang Wiryadi, and I. G. Adi Susila, "Analisis Perilaku Hubungan Pelat-Kolom Tepi Struktur Pelat Datar menggunakan Concrete Damage Plasticity (CDP) dalam Abaqus," vol. 5, no. 2, 2017 [Online]. Available: <https://ojs.unud.ac.id/index.php/jsn/article/view/32932>
- [24] L. Qingfu, G. Wei, and K. Yihang, "Parameter calculation and verification of concrete plastic damage model of ABAQUS," in *IOP Conference Series: Materials Science and Engineering*, Institute of Physics Publishing, May 2020.
- [25] E. Hognestad, "Equation for the Stress-Strain Curve of Concrete," vol. 61, no. 3, 1964.
- [26] Livermore Software Technology Corporation, "Hourglass (HG) Modes Hourglassing Avoiding or Minimizing Hourglass Modes," pp. 1–7, 2012.
- [27] A. Earij, "Nonlinear three-dimensional finite-element modelling of reinforced-concrete beams: Computational challenges and experimental validation," *Eng Fail Anal*, vol. 82, pp. 92–115, 2017.
- [28] S. P. MacHmoed, T. Tavio, and I. G. P. Raka, "Potential of new innovative confinement for square reinforced concrete columns," in *Journal of Physics: Conference Series*, 2020.
- [29] H. Elbakry, T. Ebeido, E. T. M. El-Tony, and M. Ali, "Behavior of Square RC Short Columns with New Arrangement of Ties Subjected to Axial Load: Experimental and Numerical Studies," vol. 66, no. 2, pp. 367–383, Mar. 2022.